Novel Electrochemical Sensor Based on MnO2 Nanowire Modified Carbon Paper Electrode for Sensitive Determination of Tetrabromobisphenol A

Chunmao Zhu , Qi Wu , Fanshu Yuan , Jie Liu , Dongtian Wang , Qianli Zhang *

Posted Date: 26 June 2023

doi: 10.20944/preprints202306.1791.v1

Keywords: Tetrabromobisphenol A; MnO2; Carbon paper; Modified electrode

Article

Novel Electrochemical Sensor Based on Mno2 Nanowire Modified Carbon Paper Electrode for Sensitive Determination of Tetrabromobisphenol A

Chunmao Zhu, Qi Wu, Fanshu Yuan, Jie Liu, Dongtian Wang and Qianli Zhang *

School of the Chemistry and Life Sciences, Suzhou University of Science and Technology, Suzhou 215009, China; zcm2468260200@163.com (C. Z); wq1213857@163.com (Q.W.); yuanfanshute@126.com (F.Y.); jliu12@126.com (J.L.); dongtianw@163.com (D.W.)

* Correspondence: ; zqlmhb@163.com (Q.Z.)

Abstract: In this paper, M nO2 nanowire (MnO_2-NW) modified carbon paper (CP) electrode was developed as a novel electrochemical sensor for sensitive determination of tetrabromobisphenol A (TBBPA). MnO_2 nanowire was prepared by a hydrothermal synthesis method, and the morphology and structure of MnO_2 were characterized using scanning electron microscopy, X-ray diffraction and X-ray photoelectron spectroscopy. Electrochemical performance of TBBPA on MnO_2-NW/CP was investigated by cyclic voltammetry, and the result confirmed that MnO_2-NW/CP exhibited excellent sensitive for the determination of TBBPA due to the high specific surface area and good electrical conductivity of the nanowire-like MnO_2. Moreover, the important electrochemical factors such as pH value, incubation time and modified material proportion were systematically studied to improve the determination sensitivity. The interferences from similar structure compounds on TBBPA have also been investigated. Under the optimal conditions, MnO_2-NW/CP displayed the linear range of 70 ~ 500 nM for TBBPA with the detection limit of 3.1 nM, which was superior to some electrochemical methods in references. The work presents a novel and simple method for the determination of TBBPA.

Keywords: Tetrabromobisphenol A; MnO_2; Carbon paper; Modified electrode

1. Introduction

Tetrabromobisphenol A (TBBPA), an organic compound with the chemical formula $C_{15}H_{12}Br_4O_2$, is widely used as a reactive flame retardant in electronic equipment, furniture, plastics and textiles products [1,2]. TBBPA accounts 80% of the global demand in Asia. However, TBBPA is continuously released into environment because of its massive use, releasing from the industrial products, and transformed by terrestrial and marine food chain migration [3–5]. TBBPA is a potential persistent organic pollutant reported to be bioaccumulative and highly toxic. Chronic exposure to TBBPA can induce immune, reproductive and neurotoxic effects in animal bodies [6–8]. In 2017, the World Health Organization's International Agency for Research on Cancer published a preliminary list of carcinogens for reference, and tetrabromobisphenol A is in the list of carcinogens in category 2A. Therefore, detecting TBBPA quickly and accurately is important for environmental monitoring and protection of human health.

Several analytical methods have been reported for the detection of TBBPA, including chromatographic [9,10], spectroscopic [11,12] and immunoassay methods [13,14]. For example, Hou X. et al. developed a high-performance liquid chromatography method coupled with triple quadrupole mass spectrometry (HPLC-MS/MS) with atmospheric pressure chemical ionization (APCI) source for simultaneous detection of TBBPA and its ten derivatives in determining complicated environmental samples, including sewage sludge, river water and vegetable samples. Although these methods have the good selectivity and high detection sensitivity, they are limited by the high costs of instrument maintenance, sophisticated operating skills, and extensive organic

solvents consumption. Many researchers pay attention to electrochemical sensors due to its high efficiency, low cost, prominent sensitivity, and rapid detection speed [15–17]. Presently, some electrochemical sensors have been reported for the detecting of TBBPA in environment. Nonetheless, some TBBPA electrochemical sensors' utility is limited by the non-conductive film that forms on the electrode surface due to TBBPA's electrochemical oxidation, impairing detection stability [18].

The materials used for electrode modification play a pivotal role in mitigating the passivation induced by TBBPA oxidation products. The conception and advancement of nanomaterials have considerably influenced electrochemical sensors, with their properties largely being a function of their microstructure and form. A variety of nanomaterials, such as metal oxides, carbon-based materials, metal-organic frameworks, and nanocomposites, are being studied for TBBPA detection. Zhou et al. [19] prepared a conductive composite of carbon nanotubes@zeolitic imidazole framework-67 (CNTs@ZIF-67), which possesses an excellent adsorption capacity (92.12 mg g^{-1}) for TBBPA. The composite was used to modify an acetylene black electrode for the sensitive determination of TBBPA in spiked rain and pool water samples with the aid of perfluorodecanoic acid. The sensor is stable, reproducible, and has a linear range of 0.01–1.5 μM TBBPA concentration, with a 4.2 nM detection limit (at S/N = 3). Recently, carbon dots (CDs) have attracted a lot of attention due to their low toxicity, biocompatibility and good electrical conductivity, and are widely used in biosensor, photocatalysis, electrocatalysis and electrochemical sensor. Guo et al. [20] developed magnetic CDs composed of carbon dots (CDs) and Fe_3O_4 nanoparticles via an amination reaction. A glassy carbon electrode modified with magnetic CDs and cetyltrimethylammonium bromide (CTAB) was employed as an electrochemical sensor for TBBPA detection in beverages. Magnetic CDs facilitate TBBPA oxidation, and CTAB's hydrophobic effect can enrich TBBPA. The combined impact of Magnetic CDs and CTAB boosts electrochemical sensor performance, indicating a linear range between 1 and 1000 nM, a detection limit of 0.75 nM, and displaying benefits such as rapidity, superior sensitivity, and robust stability. MXene, a kind of exceptional electrode modification material, is a two-dimensional transition metal carbide obtained by etching aluminium in Ti_3AlC_2 with hydrofluoric acid. The combination of precious metals nanoparticle and Mxene can take advantage of the extraordinary electrocatalytic properties of noble metal nanomaterials and the specific surface area and electrical conductivity of MXene. Shao et al. [21] developed a TBBPA electrochemical sensor by modifying to a glassy carbon electrode with the MXene/Au nanocomposite. The finalized sensor exhibited excellent linearity for TBBPA concentrations between 0.05 and 10 nM, a detection limit of 0.0144 nM, and successfully detected TBBPA in water, with recoveries ranging from 97.1 to 106% for the added standards. Lu et. al. [22] reported that the composite of graphitic carbon nitride (g-C_3N_4) and N-butylpyridinium hexafluorophosphate (NBH) could promote the oxidation of TBBPA. The detection of TBBPA was fulfilled using g-C_3N_4-NBH modified carbon paste electrode in the range of 1 nM to 30 nM and 30 nM to 500 nM with the limit of 0.4 nM.

Various metal oxides, including CuO, Fe_3O_4, and Fe_2O_3, have found extensive application in electrochemical sensors due to their distinct morphology [23–25]. Zhou and colleagues [23] produced different forms of CuO nanomaterials, namely nanostrips, nanowires, and microspheres. These were combined with graphene nanoplates and used to modify the surface of glassy carbon electrodes for electrochemical detection of both glucose and TBBPA. The composite made from CuO nanostrips demonstrated the most significant active surface area, the least charge transfer resistance, and the highest detection sensitivity. The designed electrochemical sensor offered sensitive TBBPA detection within a linear range of 5 to 600 nM, with an anticipated detection limit of 0.73 nM based on a signal-to-noise ratio of three. Luo et al. [24] developed an Fe_3O_4-activated biochar using surplus sludge, leading to the successful creation of an electrochemical sensor for TBBPA detection. The results from electrochemical tests suggested that the Fe_3O_4–activated biochar film possessed a more substantial active surface area, reduced charge transfer resistance, and increased TBBPA accumulation efficiency. The sensor exhibited solid linearity for TBBPA concentrations ranging from 5 to 1000 nM, a reasonably low detection limit of 3.2 nM, and was effectively utilized to determine TBBPA in water samples. Zhang et. al. [25] synthesized different morphologies of Fe_2O_3 nanomaterials such as nanoplate, nanorod and flower-like by a hydrothermal method. Electrochemical activity of Fe_2O_3

 doi:10.20944/preprints202306.1791.v1

nanomaterials modified electrodes were found to be closely related with Fe_2O_3's morphology. The composite of flower-like Fe_2O_3 (f-Fe_2O_3) and expanded graphite (EG) exhibited the largest electrochemical active area and the lowest electron transfer resistance. The f-Fe_2O_3/EG modified electrode display the best sensing performance of TBBPA with a detect limit of 1.23 nM.

Nano manganese dioxide (MnO_2) were widely used as electrode materials owing to its extraordinary electrochemical performance, low cost, abundant storage, non-toxic nature and simplicity in preparation. Currently, MnO_2 nanomaterials show promising potential in solar cell devices, bioapplications, sensing, dye mineralization etc because MnO_2 can be easily tuned into desired structure and morphology [26]. Different morphological MnO_2 nanoparticles prepared under specific conditions display varying electrochemical characteristics, boasting qualities such as excellent electrical conductivity, stability, sensitivity [27–29]. Yu et al [29] prepared a novel manganese dioxide-graphene nanosheets (MnO_2-GNSs) by a one-step hydrothermal method. A MnO_2-GNSs modified glassy carbon electrode was employed for the sensitive detection of hydrogen peroxide. Yakubu et al. [30] introduced a novel competitive electrochemical immunosensor built on gold palladium bimetallic nanoparticles for quick and sensitive detection of TBBPA in environmental water. The nanoparticles were successfully synthesized and modified with amine functionalized nanoflower-like manganese oxide. Under the best conditions, the competitive sensors demonstrated superb performance, including commendable sensitivity (LOD, 0.10 ng/mL; S/N=3) and satisfactory accuracy (recovery rate, 84-120%). This proposed method has been applied in the analysis of TBBPA from various water sources, demonstrating significant potential for the sensitive detection of trace amounts of TBBPA in aquatic settings. However, a non-enzymatic electrochemical sensor for the detection of TBBPA based on MnO_2 nanowire modified electrode has not been reported.

In this work, an easy-to-use and sensitive electrochemical sensor, a MnO_2 nanowire modified carbon paper electrode, was fabricated for the sensitive detection of TBBPA. Carbon paper (CP) is a kind of rigidity material by composing a complex and tortuous fibrous structure with a resin [31]. It is well known that the electrochemical behavior of sensors depends on their surface properties. Compared with other conventional electrodes, carbon paper electrodes possess some unique characteristics such as mechanical strength, adjustable size, porosity, conductivity and mechanical strength [32,33]. In addition, the use of carbon paper electrodes eliminates the tedious electrode grinding of solid electrode, making miniaturization and portability possible, and advancing on-line and in-situ measurements for electrochemical testing. The effects of pH, the usage of MnO_2, and the enrichment time were also studied to enhance the detection performance of MnO_2-NW/CP for the detection of TBBPA.

2. Materials and Methods

2.1. Chemicals and instruments

The carbon paper (CP) used in this research was purchased from Toray (Japan). TBBPA and Potassium ferricyanide ($K_3[Fe(CN)_6]$) were purchased from Aladdin Reagent Co. Ltd (Shanghai, China). Potassium permanganate, sodium dihydrogen phosphate (NaH_2PO_4), dibasic sodium phosphate (Na_2HPO_4), N, N-Dimethylformamide (DMF), anhydrous ethanol and acetonitrile were purchased from Jiangsu Qiangsheng Functional Chemistry Co. Ltd (Nanjing, China). All the chemicals were of analytical grade and used without further purification. All of the aqueous solutions were prepared with twice-distilled water throughout the whole experiments. The experimental temperatures were all at room temperature.

All electrochemical experiments including differential pulse voltammetry (DPV) and cyclic voltammetry (CV) were carried out in an electrochemical workstation RST 3000 with a three-electrode system. CP or modified electrode was used as the working electrode, and Ag/AgCl and Pt wire were used as the reference electrode and the auxiliary electrode, respectively.

2.2. Fabrication of manganese dioxide

Manganese dioxide was prepared by two methods.

Preprints (www.preprints.org) | NOT PEER-REVIEWED | Posted: 26 June 2023 doi:10.20944/preprints202306.1791.v1

Method 1: 0.728 g of potassium permanganate was added to a mixture solution of 80 mL H_2O and 15 mL ethanol, and then stirred at 25℃ for 2 h. After the reaction was completed, the product was washed 3 times with deionized water and anhydrous ethanol, and dried in an oven at 60℃ for 12 h [34].

Method 2: 0.45 g of potassium permanganate was dissolved into 30 mL of 0.4 M acetic acid solution, transferred to a 50 mL hydrothermal reactor and kept at 140°C for 12 h. After the reaction was completed, the product was washed 3 times with deionized water and anhydrous ethanol, and dried in an oven at 60℃ for 12 h.

2.3. Preparation of modified electrodes

The CP was cut into 1×0.5 cm and ultrasonically cleaned in ethanol for five minutes. To excite the electrochemical properties of the CP [35], the electrode was immersed in 0.1 M sulfuric acid solution and scanned for 50 cycles from -0.2 V to 1.0 V at 100 mV/s using the CV method. Then, the electrode was cleaned with deionized water and dried at room temperature.

4.0 mg of manganese dioxide was dispersed in 2.0 mL of DMF solution with the aid of an ultrasonic bath to obtain a suspension of 2 mg/mL of manganese dioxide. 7.0 μL of the above suspension was dropped onto the surface of the treated carbon paper electrode and dried at room temperature.

3. Results and discussion

3.1. Characterization of manganese dioxide

Scanning electron microscope (SEM) images was used to investigate the microstructures and morphologies of MnO_2 nanomaterials. Different microstructures and morphologies of MnO_2 nanomaterials were found when MnO_2 was prepared by different methods. As shown in Figure 1a, irregular sheet structure was obtained when MnO_2 was synthesized by reducing potassium permanganate using ethanol as a reducing agent under normal temperature and pressure at pH 7 (method 1). MnO_2 nanowire (Figure 1b) was observed when MnO_2 was prepared via a hydrothermal synthesis under acidic conditions (method 2). The length of nanowire is approximate 6–10 μm. The obvious different morphologies were expected to resulted in different electrochemical performance. The crystal structure of MnO_2 nanowire (MnO_2-NW) was characterized with X-ray powder diffraction (XRD). In XRD patterns of MnO_2-NW (Figure 1c), the diffraction peaks at 12.78°,18.06°, 28.82°, 37.82° and 42.17° are indexed to crystal Surface of (110), (200), (310), (211) and (301), respectively, which are matched with the standard diffraction pattern of α-MnO_2 (JCPDS card No.44-0141). More importantly, no other impurities are founded from these XRD patterns, revealing that as-synthesized MnO_2-NW is well crystallized and at high purity.

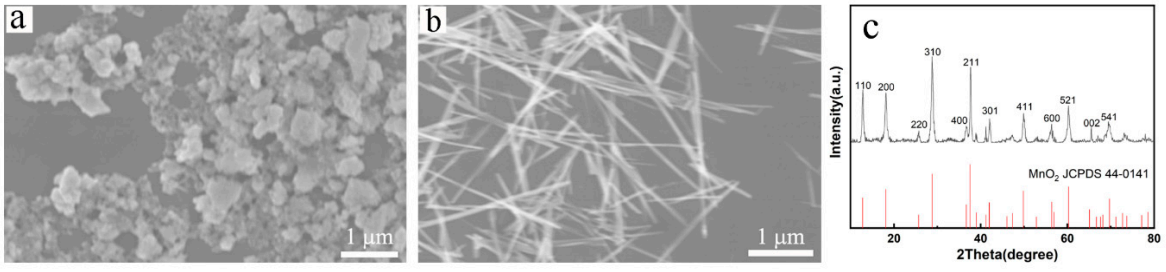

Figure 1. SEM of granular MnO_2(a) and MnO_2-NW(b); XRD of MnO_2-NW(c).

X-ray photoelectron spectroscopy (XPS) was used to study the surface composition of MnO_2-NW (Figure 2). According to the full scan XPS spectrum (Figure 2a), Mn and O were observed on the surface of the sample of MnO_2-NW. In the high-resolution spectrum of O 1s (Figure 2b), the peak at 529.88 eV corresponded to lattice oxygen, and the appearance of a high-intensity peak indicates that a large amount of lattice oxygen (Olatt) was present in MnO_2 nanowires. The characteristic peak of

Preprints (www.preprints.org) | NOT PEER-REVIEWED | Posted: 26 June 2023 doi:10.20944/preprints202306.1791.v1

Oabs at 531.49 eV was related to surface-adsorbed oxygen, hydroxyl groups, or defect-related oxygen species [36,37]. Figure 2c displayed the XPS energy spectrum of Mn 3s. The valence state of Mn was usually determined based on the peak spacing of Mn 3s. The peak spacing of Mn 3s in MnO_2-NW was 4.70 eV, indicating that most of the Mn in the sample exists in the form of +4 valence. In XPS spectra of Mn 2p (Figure 2d), the peaks at 642.47 eV and 641.04 eV correspond to Mn^{4+} and Mn^{3+}, respectively. The content of Mn^{3+} is relatively low, indicating that most of the Mn in MnO_2-NW samples exist in the form of +4 valence [38,39].

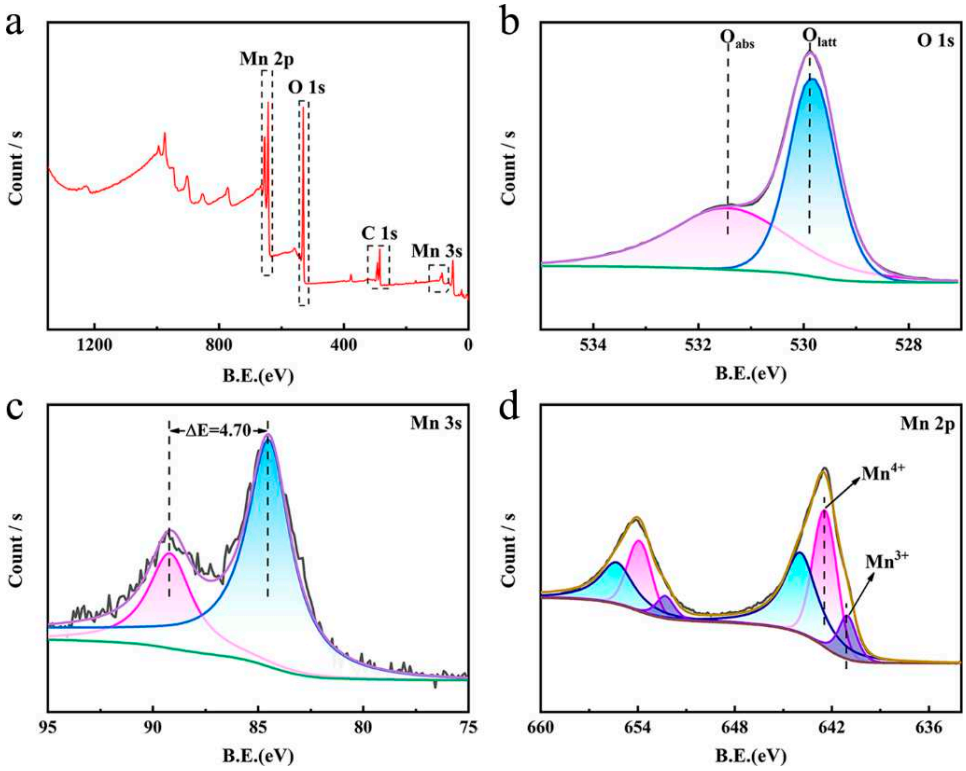

Figure 2. XPS figures of MnO_2-NW. (a) full spectrum, (b) O 1s, (c) Mn 3s, (d) Mn 2p.

3.2. Electrochemical behavior of TBBPA on MnO_2-NW/CP

Figure 3a showed the cyclic voltammograms of 500 nM TBBPA on CP, MnO_2/CP (MnO_2 nanosheet), and MnO_2-NW/CP, respectively. The buffer solution was 0.10 M phosphate buffer solution (pH 6.5). As can be seen from Figure 3a, an irreversible oxidation peak at 0.60 V (*vs*. Ag/AgCl) was found to be corresponding to the irreversible oxidation of TBBPA at the working electrode surface. The comparation of the oxidation peak current of TBBPA on the above three electrodes was displayed in Figure 3b. It was shown that the oxidation peak current of TBBPA was slightly enhanced by modifying nanosheet MnO_2 on CP, and the electrochemical signal of TBBPA on MnO_2-NW/CP was approximately twice higher than that on the bare CP electrode. Furthermore, the oxidation potential shifted to be 0.58 V. Thus, the electrochemical performance of MnO_2 modified electrodes was influenced largely by the morphology of MnO_2 nanomaterials. The oxidation of TBBPA was obvious promoted when CP electrode was modified by MnO_2-NW, which may be due to the larger specific surface area and better electrical conductivity of MnO_2-NW. Hence, MnO_2-NW/CP were chosen for the detection of TBBPA.

Preprints (www.preprints.org) | NOT PEER-REVIEWED | Posted: 26 June 2023 doi:10.20944/preprints202306.1791.v1

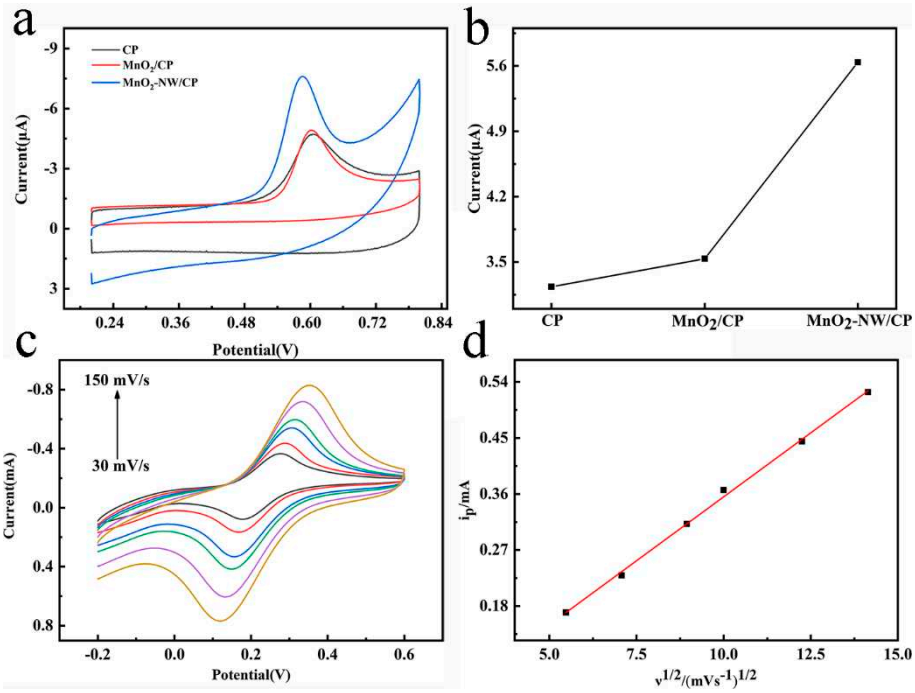

Figure 3. (a) CVs of 500 nM TBBPA on different electrodes; (b) oxidation current of TBBPA on different electrodes; (c) CVs of MnO_2-NW/CP in 2.5 mM $K_3[Fe(CN)_6]$ at different scan rates; (d) The linear plot of $K_3[Fe(CN)_6]$ ipa vs. $\upsilon^{1/2}$.

CVs of MnO_2-NW/CP in 0.1 M KCl solution containing 2.5 mM $K_3[Fe(CN)_6]$ at various scan rates was recorded in the range of 30–150 mV/s to investigate the effective electrochemical area of MnO_2-NW/CP electrode. It was observed that the oxidation and reduction peaks of potassium ferricyanide increase with increasing scanning speed at MnO_2-NW/CP electrode, and the potential difference between the oxidation and reduction peaks becomes larger. The diffusion-controlled kinetics of $K_3[Fe(CN)_6]$ could be deduced from the linear relationship between oxidation peak currents ip and square root of scan rates $\upsilon^{1/2}$ with the regression equation of ip = $0.04109\upsilon^{1/2}$–0.05549 (R^2=0.9976) (Figure 3d). The Randles-Sevcik equation was used to calculate the effective surface area (ESA) [40].

$$i_p = 0.4463nFAC\left(\frac{nF\upsilon D}{RT}\right)^{1/2} = 2.69\times10^5 n^{2/3}ACD^{1/2}\upsilon^{1/2} \quad (25℃) \quad (1)$$

Where ip (A) is the oxidation or reduction peak current; n is the total number of electrons exchanged in the redox reaction, A (cm^2) is the effective surface area; C (mol/cm^3) is the concentration of $K_3[Fe(CN)_6]$ (2.5 mM); D (cm^2/s) is the diffusion coefficient of $[Fe(CN)_6]^{3-}$ (6.5×10^{-6} cm^2/s) and υ (V/s) is the scan rate. In our experiment, the slope was 0.04109, and the ESA value was calculated to be 0.24 cm^2, which was about 9 times larger than that of bare CP.

Figure 4a showed CVs of MnO_2-NW/CP in 0.1 M pH 6.5 phosphate buffer solutions containing 500 nM TBBPA at different scan rates in the range of 25–150 mV/s. As the scan rate increased, the oxidation peak currents of TBBPA kept increasing. Figure 4b showed a plot of TBBPA oxidation peak current versus sweep rate with the linear equation ip=0.0975υ + 0.00459 (R^2 = 0.9915), and Figure 4c was a plot of ip versus $\upsilon^{1/2}$ with the linear equation ip=$1.67755\upsilon^{1/2}$–6.61462 (R^2 = 0.9531). Thus, the oxidation peak currents of TBBPA increase linearly with the scan rates, demonstrating that TBBPA oxidation on a MnO_2-NW/CP is an adsorption-controlled process. Moreover, the oxidation peak potentials of TBBPA were found to shift toward positive potentials with the increase of scan rates.

Preprints (www.preprints.org) | NOT PEER-REVIEWED | Posted: 26 June 2023 doi:10.20944/preprints202306.1791.v1

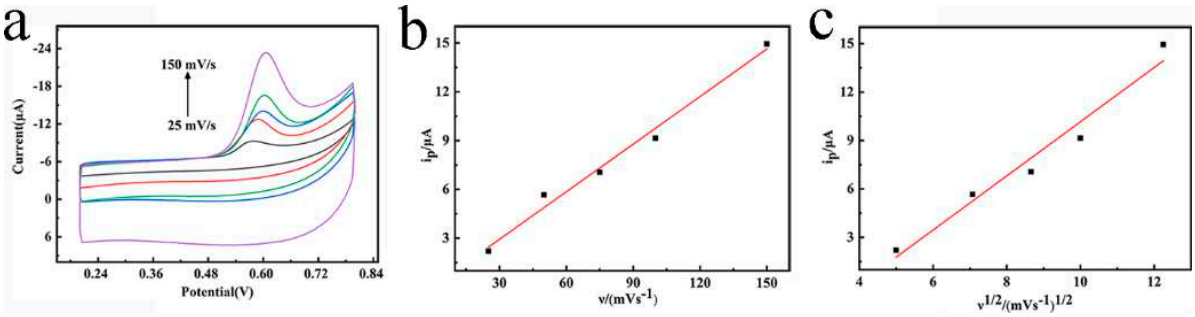

Figure 4. (a) CVs of 500 nM TBBPA in 0.1 M pH 6.5 PBS on MnO_2-NW/CP at different scan rates; (b)The linear plot of ip vs. υ; (c)The linear plot of ip vs. $υ^{1/2}$.

3.3. Optimization of experimental conditions

DPV was chosen to prepare a sensitive sensor for the determination of TBBPA. The experiment parameters including the pH value of buffer solution, the enrich time and the amount of MnO_2-NW were optimized by recording the electrochemical performance of TBBPA under different experiment conditions.

Figure 5a shows the oxidation peak currents and peak potentials of TBBPA at different pH conditions. It was found that the oxidation peak currents of TBBPA increased with increasing pH in the range of 5.5–6.5, and reached a maximum at pH 6.5. The pKa_1 and pKa_2 of TBBPA were reported to be 7.5 and 8.5. TBBPA was not dissociated when pH was 6.5. The undissociated TBBPA can easily adsorbed on MnO_2-NW/CP electrode than that of dissociated form, which resulted in the maximum oxidation peak current of TBBPA at pH 6.5. Hence, pH 6.5 was chosen as the optimum pH condition in the subsequent experiments. In the pH range of 5.8–8.0, the oxidation peak potential of TBBPA negatively linear shifted with an increase of pH value following the equations of Ep = 0.978–0.0594pH, showing that protons took part in the electrochemical reaction of TBBPA. The slope -0.0594 V/pH was close to the value obtained from the Nernst equation (-0.059 V/pH), which indicated that the number of electrons equal to the number of protons during the oxidation of TBBPA [41].

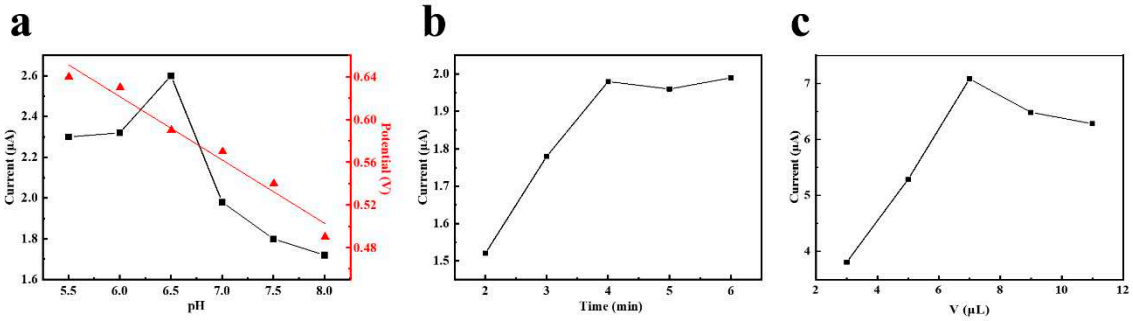

Figure 5. (a) The effect of pH on the oxidation peak current and potential of TBBPA; (b) The effect of enrichment time on the peak current of TBBPA; (c) The effect of MnO_2-NW amount on the peak current of TBBPA.

The effect of enrichment time on the oxidation peak current of TBBPA (500 nM) was shown in Figure 5b. When the enrichment time was less than 5 min, the peak current increases rapidly with the increase of enrichment time because more TBBPA was adsorbed on MnO_2-NW/CP electrode with increasing of enrich time. When the enrichment time was above 5 min, the oxidation peak current tends to be stable due to adsorption saturation of TBBPA. Therefore, 5 min of enrichment time was chosen.

The effect of modification amount of MnO_2-NW was investigated in Figure 5c. It was found that the oxidation current of TBBPA increased sharply when the modification amount of MnO_2-NW suspension increased from 3.0 to 7.0 μL. This might be resulted from more catalyst enhanced catalytic

Preprints (www.preprints.org) | NOT PEER-REVIEWED | Posted: 26 June 2023 doi:10.20944/preprints202306.1791.v1

ability. However, when the modification amount was over 7.0 μL, the oxidation peak current decreased due to the fact of the thicker modification layer, which was easy to cover some active sites. Therefore, 7.0 μL suspension of MnO_2-NW was selected as the optimal modification amount in this work.

3.4. Electrochemical detection of TBBPA

DPV of MnO_2-NW/CP in different TBBPA concentrations were investigated under the optimal experimental conditions (Figure 6). As shown in Figure 6a, the oxidation currents increased when TBBPA was added successively from 70 to 500 nM. The linear regression equation was ip = 0.00323c + 0.06304, R^2 = 0.9914 (Figure 6b). The estimated detection limit is 3.1 nM based on a three-signal-to-noise ratio of 3. It could be seen that our electrochemical sensor exhibited a wide linear range and a low detection limit, which might due to the high ESA of the MnO_2-NW/CP, plenty of active sites. Our experimental results were compared with the literature reports in Table 1, indicating that this method has some favorable advantages.

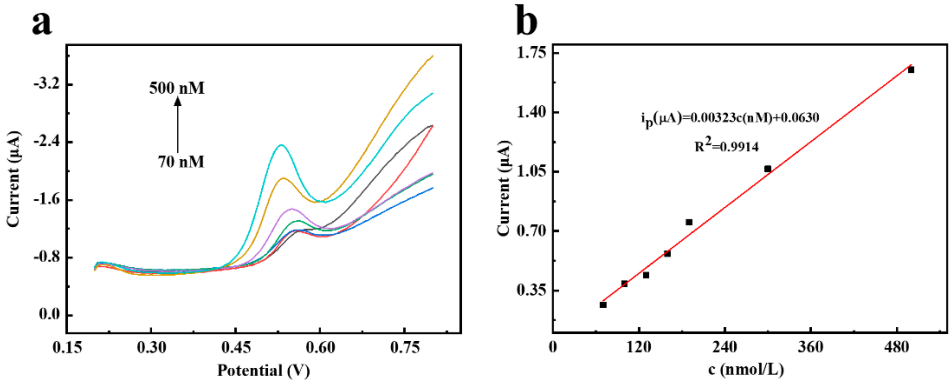

Figure 6. (a) DPVs of MnO_2-NW/CP in 0.1 M pH 6.5 PBS containing different concentrations of TBBPA; (b) The corresponding calibration plots between the peak currents and the concentrations of TBBPA.

Table 1. Comparison of the experimental results with other electrodes or methods.

Sensor assembly	Method	LOD	Linear range	Reference
CNTs@ZIF-67/PFDA/AB	DPV	4.2 nM	10 ~ 150 nM	[19]
AuNPs-PSSA/GCE	DPV	25 pM	0.1 ~ 10 nM	[42]
MI-TiO_2/Au/rGO	DPV, CV	0.51 nM	1.68 ~ 100 nM	[43]
CTAB-MnO_2/Pd	I-t	0.17 ng/mL	0 ~ 81 ng/mL	[44]
poly(PPBim-DS)/GCE	DPV	20 nM	0.05 ~ 10 μM	[39]
MnO_2-NW/CP	DPV	3.1 nM	70 ~ 500 nM	This work

Five parallel MnO_2-NW/CP electrodes were prepared for the detection of 500 nM TBBPA, and the detection relative standard deviation was 3.8%. One of the above five electrodes was further investigated for five consecutive times, and the relative standard deviation was 1.9%. The results showed good reproducibility and precision of MnO_2-NW/CP.

3.5. Real samples analysis

To estimate the potential of a MnO_2-NW for the detection of TBBPA in practical applications, the fabricated electrochemical sensor was employed to detect TBBPA in real lake water. (Suzhou, China). Before detection, the water was filtered through a 0.45 μm membrane to remove the suspended solids. No response of TBBPA was found in these real samples, indicating that the concentration of TBBPA was extremely low or no TBBPA was existed in these real samples. Then standard solutions of TBBPA were spiked into real sample solutions for the recovery evaluation. The recoveries were in the range of 94.5% to 100.5%. The results indicated that MnO_2-NW/CP is reliable and could be applied to detect TBBPA in the actual water sample.

4. Conclusions

In this study, a cost effective, simple fabricated and sensitive electrochemical sensor was prepared by modifying carbon paper with MnO_2 nanomaterial. The performance of electrochemical sensors was proven to be closely corresponded to the microscopic morphology of MnO_2. The fabricated MnO_2-NW/CP displayed attractive performance for the detection of TBBPA. The sensitivity and stability of MnO_2-NW/CP were satisfied, and the selectivity of MnO_2-NW/CP can be further enhanced by combining other materials such as molecular imprinting technology. It is reasonable to believe that MnO_2 nanowire-based electrochemical sensor might be a promising method for the effective detection of TBPPA in environment monitoring.

Author Contributions: Conceptualization, Q.Z.; methodology, Q.Z. and C.Z.; software, C.Z.; validation, Q.W.; investigation, C.Z; resources, Q.Z.; data curation, C.Z. and F.Y.; writing—original draft preparation, C.Z.; writing—review and editing Q.Z., J. L. and D.W.; funding acquisition, Q.Z. All authors have read and agreed to the published version of the manuscript.

Funding: This work was financially supported by the National Natural Science Foundation of China (No.20905055), Postgraduate Research & Practice Innovation Program of Jiangsu Province (No.SJCX22_1564).

Conflicts of Interest: The authors declare no conflict of interest.

References

1. Lee, S.; Song, G. J.; Kannan, K.; Moon, H. B., Occurrence of PBDEs and other alternative brominated flame retardants in sludge from wastewater treatment plants in Korea. *Sci. Total Environ.* **2014,** *470*, 1422-1429.
2. Shi, Z. X.; Zhang, L.; Li, J. G.; Wu, Y. N., Legacy and emerging brominated flame retardants in China: A review on food and human milk contamination, human dietary exposure and risk assessment. *Chemosphere* **2018,** *198*, 522-536.
3. Shi, Z. X.; Zhang, L.; Zhao, Y. F.; Sun, Z. W.; Zhou, X. Q.; Li, J. G.; Wu, Y. N., Dietary exposure assessment of Chinese population to tetrabromobisphenol-A, hexabromocyclododecane and decabrominated diphenyl ether: Results of the 5th Chinese Total Diet Study. *Environ. Pollut.* **2017,** *229*, 539-547.
4. Wluka, A.; Wozniak, A.; Wozniak, E.; Michalowicz, J., Tetrabromobisphenol A, terabromobisphenol S and other bromophenolic flame retardants cause cytotoxic effects and induce oxidative stress in human peripheral blood mononuclear cells (in vitro study). *Chemosphere* **2020,** *261*, 127705.
5. Zuiderveen, E. A. R.; Slootweg, J. C.; de Boer, J., Novel brominated flame retardants—A review of their occurrence in indoor air, dust, consumer goods and food. *Chemosphere* **2020,** *255*, 126816.
6. Nakajima, A.; Saigusa, D.; Tetsu, N.; Yamakuni, T.; Tomioka, Y.; Hishinuma, T., Neurobehavioral effects of tetrabromobisphenol A, a brominated flame retardant, in mice. *Toxicol. Lett.* **2009,** *189* (1), 78-83.
7. Feiteiro, J.; Mariana, M.; Cairrao, E., Health toxicity effects of brominated flame retardants: From environmental to human exposure. *Environ. Pollut.* **2021,** *285*, 117475.
8. Jagic, K.; Dvorscak, M.; Klincic, D., Analysis of brominated flame retardants in the aquatic environment: a review. *Arh Hig Rada Toksiko* **2021,** *72* (4), 254-267.
9. Gao, W.; Li, G. L.; Liu, H.; Tian, Y.; Li, W. T.; Fa, Y.; Cai, Y. Q.; Zhao, Z. S.; Yu, Y. L.; Qu, G. B.; Jiang, G. B., Covalent organic frameworks with tunable pore sizes enhanced solid-phase microextraction direct ionization mass spectrometry for ultrasensitive and rapid analysis of tetrabromobisphenol A derivatives. *Sci. Total Environ.* **2021,** *764*, 144388.
10. Zhang, S.; Liu, J.; Hou, X.; Zhang, H.; Zhu, Z.; Jiang, G.,. Sensitive method for simultaneous determination of TBBPA and its ten derivatives. *Talanta,* **2023**, 124750.
11. Zeng, L. S.; Cui, H. R.; Chao, J. L.; Huang, K.; Wang, X.; Zhou, Y. K.; Jing, T., Colorimetric determination of tetrabromobisphenol A based on enzyme-mimicking activity and molecular recognition of metal-organic framework-based molecularly imprinted polymers. *Microchem. J.* **2020,** *187* (2), 142.

12. Yanagisawa, H.; Sasaki, K.; Sasaki, Y.; Omata, A.; Ichino, R.; Fujimaki, S., Photometric Screening of Tetrabromobisphenol A in Resin Using Iron(III) Nitrate/Hexacyanoferrate(III) Mixture as a Colorimetric Reagent. *Anal Sci* **2021,** *37* (12), 1815-1819.
13. Fu, H. J.; Wang, Y.; Xiao, Z. L.; Wang, H.; Li, Z. F.; Shen, Y. D.; Lei, H. T.; Sun, Y. M.; Xu, Z. L.; Hammock, B., A rapid and simple fluorescence enzyme-linked immunosorbent assay for tetrabromobisphenol A in soil samples based on a bifunctional fusion protein. *Ecotoxicol. Environ. Saf.* **2020,** *188*, 109904.
14. Li, Z. F.; Wang, Y.; Vasylieva, N.; Wan, D. B.; Yin, Z. H.; Dong, J. X.; Hammock, B., An Ultrasensitive Bioluminescent Enzyme Immunoassay Based on Nanobody/Nanoluciferase Heptamer Fusion for the Detection of Tetrabromobisphenol A in Sediment. *Anal. Chem.* **2020,** *92* (14), 10083-10090.
15. Chen, H. J.; Zhang, Z. H.; Cai, R.; Rao, W.; Long, F., Molecularly imprinted electrochemical sensor based on nickel nanoparticles-graphene nanocomposites modified electrode for determination of tetrabromobisphenol A. *Electrochim. Acta* **2014,** *117*, 385-392.
16. Zhang, Z. H.; Cai, R.; Long, F.; Wang, J., Development and application of tetrabromobisphenol A imprinted electrochemical sensor based on graphene/carbon nanotubes three-dimensional nanocomposites modified carbon electrode. *Talanta* **2015,** *134*, 435-442.
17. Zhou, T. T.; Feng, Y. Q.; Zhou, L. X.; Tao, Y.; Luo, D.; Jing, T.; Shen, X. L.; Zhou, Y. K.; Mei, S. R., Selective and sensitive detection of tetrabromobisphenol-A in water samples by molecularly imprinted electrochemical sensor. *Sens. Actuators B Chem.* **2016,** *236*, 153-162.
18. Wang, Y. Y.; Liu, G. S.; Hou, X. D.; Huang, Y. N.; Li, C. Y.; Wu, K. B., Assembling gold nanorods on a poly-cysteine modified glassy carbon electrode strongly enhance the electrochemical reponse to tetrabromobisphenol A. *Microchim Acta* **2015,** *183* (2), 689-696.
19. Zhou, T. T.; Zhao, X. Y.; Xu, Y. H.; Tao, Y.; Luo, D.; Hu, L. Q.; Jing, T.; Zhou, Y. K.; Wang, P.; Mei, S. R., Electrochemical determination of tetrabromobisphenol A in water samples based on a carbon nanotubes@zeolitic imidazole framework-67 modified electrode. *RSC Adv.* **2020,** *10* (4), 2123-2132.
20. Guo, J. H.; Zhou, B. Y.; Li, S. Y.; Tong, Y. Y.; Li, Z.; Liu, M. H.; Li, Y. H.; Qu, T. X.; Zhou, Q. X., Novel electrochemical sensor from magnetic carbon dots and cetyltrimethylammonium bromide for sensitive measurement of tetrabromobisphenol A in beverages. *Chemosphere* **2022,** *298*, 134326.
21. Shao, Y. M.; Zhu, Y.; Zheng, R.; Wang, P.; Zhao, Z. Z.; An, J., Highly sensitive and selective surface molecularly imprinted polymer electrochemical sensor prepared by Au and MXene modified glassy carbon electrode for efficient detection of tetrabromobisphenol A in water. *Adv Compo Hybrid Ma* **2022,** *5* (4), 3104-3116.
22. Zhao, Q., Zhou, H., Wu, W., Wei, X., Jiang, S., Zhou, T., Lu, Q. (2017). Sensitive electrochemical detection of tetrabromobisphenol A based on poly (diallyldimethylammonium chloride) modified graphitic carbon nitride-ionic liquid doped carbon paste electrode. *Electrochimica Acta* **2017**, 254, 214-222.
23. Zhou, Q.; Zhang, Y. Y.; Zeng, T.; Wan, Q. J.; Yang, N. J., Morphology-dependent sensing performance of CuO nanomaterials. *Anal. Chim. Acta* **2021,** *1171*, 338663.
24. Luo, S. X.; Yang, M. Z.; Wu, Y. H.; Li, J.; Qin, J.; Feng, F., A Low Cost Fe_3O_4-Activated Biochar Electrode Sensor by Resource Utilization of Excess Sludge for Detecting Tetrabromobisphenol A. *Micromachines* **2022,** *13* (1), 115.
25. Chen, X. Y.; Zhang, Y. Y.; Li, C.; Li, C.; Zeng, T.; Wan, Q. J.; Li, Y. W.; Ke, Q.; Yang, N. J., Nanointerfaces of expanded graphite and Fe_2O_3 nanomaterials for electrochemical monitoring of multiple organic pollutants. *Electrochim. Acta* **2020,** *329*, 135118.
26. Baral, A.; Satish, L.; Zhang, G. Y.; Ju, S. H.; Ghosh, M. K., A Review of Recent Progress on Nano MnO_2: Synthesis, Surface Modification and Applications. *J Inorg Organomet Polym Mater* **2020,** *31* (3), 899-922.
27. Yu, Y.; Liu, S. L.; Ji, J.; Huang, H. B., Amorphous MnO_2 surviving calcination: an efficient catalyst for ozone decomposition. *Catal. Sci. Technol.* **2019,** *9* (18), 5090-5099.
28. Guan, J. F.; Huang, Z. N.; Zou, J.; Jiang, X. Y.; Peng, D. M.; Yu, J. G., A sensitive non-enzymatic electrochemical sensor based on acicular manganese dioxide modified graphene nanosheets composite for hydrogen peroxide detection. *Ecotoxicol. Environ. Saf.* **2020,** *190*, 110123.
29. Huang, Z. N.; Liu, G. C.; Zou, J.; Jiang, X. Y.; Liu, Y. P.; Yu, J. G., A hybrid composite of recycled popcorn-shaped MnO_2 microsphere and Ox-MWCNTs as a sensitive non-enzymatic amperometric H_2O_2 sensor. *Microchem. J.* **2020,** *158*, 105215.
30. Yakubu, S.; Xiao, J. X.; Gu, J. P.; Cheng, J.; Wang, J.; Li, X. S.; Zhang, Z., A competitive electrochemical immunosensor based on bimetallic nanoparticle decorated nanoflower-like MnO_2 for enhanced peroxidase-like activity and sensitive detection of Tetrabromobisphenol A. *Sens. Actuators B Chem.* **2020,** *325*, 128909.
31. Torrinha, A.; Morais, S., Electrochemical (bio)sensors based on carbon cloth and carbon paper: An overview. *Trends Analyt Chem* **2021,** *142*, 116324.
32. Li, Y. H.; Xu, Q. Z.; Li, Q. Y.; Wang, H. Q.; Huang, Y. G.; Xu, C. W., Pd deposited on MWCNTs modified carbon fiber paper as high-efficient electrocatalyst for ethanol electrooxidation. *Electrochim. Acta* **2014,** *147*, 151-156.

33. Kannan, P.; Maiyalagan, T.; Marsili, E.; Ghosh, S.; Niedziolka-Jonsson, J.; Jonsson-Niedziolka, M., Hierarchical 3-dimensional nickel-iron nanosheet arrays on carbon fiber paper as a novel electrode for non-enzymatic glucose sensing. *Nanoscale* **2016,** *8* (2), 843-55.
34. Sun, H. Y.; Wang, C. X.; Xu, Y. J.; Dai, D. M.; Deng, X. Y.; Gao, H. T., A Novel Electrochemical Sensor Based on A Glassy Carbon Electrode Modified with GO/MnO_2 for Simultaneous Determination of Trace Cu(II) and Pb(II) in Environmental Water. *ChemistrySelect* **2019,** *4* (40), 11862-11871.
35. Radulescu, M. C.; Bucur, M. P.; Bucur, B.; Radu, G. L., Ester flavorants detection in foods with a bienzymatic biosensor based on a stable Prussian blue-copper electrodeposited on carbon paper electrode. *Talanta* **2019,** *199*, 541-546.
36. Tagsin, P.; Suksangrat, P.; Klangtakai, P.; Srepusharawoot, P.; Ruttanapun, C.; Kumnorkaew, P.; Pimanpang, S.; Amornkitbamrung, V., Electrochemical mechanisms of activated carbon, alpha-MnO_2 and composited activated carbon-alpha-MnO2 films in supercapacitor applications. *Appl. Surf. Sci.* **2021,** *570*, 151056.
37. Cui, Y.; Song, H. K.; Shi, Y. Y.; Ge, P. X.; Chen, M. D.; Xu, L. L., Enhancing the Low-Temperature CO Oxidation over CuO-Based alpha-MnO_2 Nanowire Catalysts. *Nanomaterials* **2022,** *12* (12), 2083.
38. Zhou, X.; Ye, X. X.; Wu, K. B.; Li, C.; Wang, Y. Y., Electrochemical sensing of terabromobisphenol A at a polymerized ionic liquid film electrode and the enhanced effects of anions. *Ionics (Kiel)* **2018,** *24* (9), 2843-2850.
39. Ganesh, A.; Sivakumar, T.; Sankar, G., Biomass-derived porous carbon-incorporated MnO_2 composites thin films for asymmetric supercapacitor: synthesis and electrochemical performance. *J. Mater. Sci. Mater. Electron.* **2022,** *33* (18), 14772-14783.
40. Shen, T. Y.; Liu, T. C.; Mo, H. Q.; Yuan, Z. C.; Cui, F.; Jin, Y. X.; Chen, X. J., Cu-based metal-organic framework HKUST-1 as effective catalyst for highly sensitive determination of ascorbic acid. *RSC Adv.* **2020,** *10* (39), 22881-22890.
41. Stradins, J.; Hasanli, B., Anodic voltammetry of phenol and benzenethiol derivatives .1. Influence of pH on electrooxidation potentials of substituted phenols and evaluation of pK(a) from anodic voltammetry data. *J. Electroanal. Chem.* **1993,** *353* (1-2), 57-69.
42. Shen, J.; Bian, C.; Xia, S. H.; Wu, K. B., Poly(sulfosalicylic acid)-functionalized gold nanoparticles for the detection of tetrabromobisphenol A at pM concentrations. *J. Hazard. Mater.* **2020,** *388*, 121733.
43. Li, Z.; Hu, J. Y.; Lou, Z. Z.; Zeng, L. X.; Zhu, M. S., Molecularly imprinted photoelectrochemical sensor for detecting tetrabromobisphenol A in indoor dust and water. *Microchem. J.* **2021,** *188* (10), 320.
44. Yakubu, S.; Jia, B. Y.; Guo, Y. J.; Zou, Y. M.; Song, N. H.; Xiao, J. X.; Liang, K. L.; Bu, Y. Q.; Zhang, Z., Indirect competitive-structured electrochemical immunosensor for tetrabromobisphenol A sensing using CTAB-MnO_2 nanosheet hybrid as a label for signal amplification. *Anal. Bioanal. Chem.* **2021,** *413* (16), 4217-4226.